AERODYNAMIC PARAMETERS OF HIGH PERFORMANCE AIRCRAFT ESTIMATED FROM WIND TUNNEL AND FLIGHT TEST DATA

Vladislav Klein
The George Washington University
Hampton, Virginia 23681

and

Patrick C. Murphy
NASA Langley Research Center
Hampton, Virginia 23681

SUMMARY

A concept of system identification applied to high performance aircraft is introduced followed by a discussion on the identification methodology. Special emphasis is given to model postulation using time invariant and time dependent aerodynamic parameters, model structure determination and parameter estimation using ordinary least squares and mixed estimation methods. At the same time problems of data collinearity detection and its assessment are discussed. These parts of methodology are demonstrated in examples using flight data of the X-29A and X-31A aircraft. In the third example wind tunnel oscillatory data of the F-16XL model are used. A strong dependence of these data on frequency led to the development of models with unsteady aerodynamic terms in the form of indicial functions. The paper is completed by concluding remarks.

NOMENCLATURE

Only the main symbols are introduced. Other symbols are explained in the body of the paper.

$\bar{c}$	mean aerodynamic chord, m
b	wing span
C_L	lift coefficient
C_ℓ, C_m, C_n	rolling-, pitching- and yawing-moment coefficient
$k=\omega\ell/V$	reduced frequency
ℓ	characteristics length, m
p, q, r	roll, pitch and yaw rate, rad/sec
R^2	coefficient of determination
V	airspeed, m/sec
α, β	angle of attack and sideslip angle, rad
η_c	control stick deflection
δ_a, δ_r	aileron and rudder deflection, rad
δ_c, δ_f, δ_s	canard, flap and strake deflection,rad
δ_{qtv}, δ_{rtv}	thrust vectoring deflection in pitch and yaw, rad
θ	unknown parameter

1. INTRODUCTION

The introduction of highly maneuverable and often inherently unstable aircraft has been presenting new challenges to aircraft identification and parameter estimation. These aircraft can perform rapid large amplitude maneuvers, often extended to the stall and poststall region where nonlinear and unsteady aerodynamic effects could be pronounced. This introduces a problem of determining how complex the model should be. Although a more complex model can be justified for more accurate description of airplane motion, it has not been clear in parameter estimation which relationship between model complexity and measurement information would be the best. If estimates for too many parameters are sought from a limited amount of data, a reduced accuracy can be expected or attempts to identify all parameters might fail. The high performance aircraft may also have more control surfaces moved through a flight control system than conventional aircraft. Such a system can introduce a close relationship between the deflections of various surfaces and at the same time can preclude maneuvers from being suitable for system identification. These characteristics can be reflected in an inability to estimate the effectiveness of individual control surfaces and to obtain accurate estimates of the remaining parameters. One of the reasons for these problems is related to the near linear relationship among several variables entering the model for various estimation techniques. This near linear relationship is often called data collinearity [1].

In recent years more attention has been given to the analysis of data obtained from dynamic wind tunnel tests. The frequency and amplitude dependency of oscillatory and ramp test data led to postulation of models with linear or nonlinear unsteady effects and subsequent parameter estimation in these models [2,3].

As follows from the above mentioned reasons and experience, a successful parameter estimation requires the

following:

a) design of an experiment for obtaining data with high accuracy, high information content and low collinearity among measured inputs and outputs;

b) determination of model structure which represents an adequate model for the aircraft under test in each maneuver analyzed;

c) introduction of techniques which reduce the adverse effect of data collinearity on parameter estimates when severe data collinearity could not be avoided by experiment design.

The purpose of this paper is to present a general approach to aircraft identification with emphasis on the above mentioned requirements for successful identification of a high performance aircraft model. The paper starts with an overview of system identification methodology followed by a discussion on data collinearity and biased estimation. In examples the flight data from experiments on X-29A and X-31A aircraft will be used. The forced oscillatory wind tunnel data on F-16XL model were selected for estimation of unsteady aerodynamic parameters. The paper is completed by concluding remarks.

2. AIRCRAFT IDENTIFICATION METHODOLOGY

When system identification is applied to an aircraft the equations governing its motion are postulated and an experiment is designed for obtaining time histories of the input and output variables. The equations of motion are formed by rigid-body force and moment equations

$$\begin{aligned} m\dot{V} + m\omega \times V &= F_G + F_T + F(V,\omega,u,\theta) \\ I\dot{\omega} + \omega \times I\omega &= G(V,\omega,u,\theta) \end{aligned} \qquad (1)$$

and by a set of kinematic equations relating the Euler (attitude) angles and angular velocities. In eq. (1) m is the mass, I is the inertia matrix, V and ω are the linear and angular velocity vectors, and u is the control vector. The vectors F_G and F_T represent the gravity and propulsion force, F and G aerodynamic force and moment respectively, and θ is a vector of parameters which specify aerodynamic characteristics of the aircraft.

For system identification, the aircraft state equations are completed by the output and measurement equations. The complete set of all these equations can be written as

$$\begin{aligned} \dot{x} &= f[x(t),u(t),\theta], \quad x(0)=x_0 \\ y &= h[x(t),u(t),\theta] \\ z(i) &= y(i) + v(i), \quad i=1,2,...,N \end{aligned} \qquad (2)$$

where the state vector, x, is comprised of V, ω and Euler angles, and u is the control vector of control surface deflections. The outputs, y, are the variables defining aircraft responses. The measured outputs, z(i), are corrupted by measurement noise, v(i), and the number of data points is N.

Aircraft identification can be defined as follows: *Aircraft identification is a determination, from input and output measurements, of a structure for* $F(\theta)$ *and* $G(\theta)$ *and estimation of unknown parameters,* θ, *in* $F(\theta)$ *and* $G(\theta)$. In many practical applications, the structure of $F(\theta)$ and $G(\theta)$ is assumed to be known and aircraft identification is reduced to parameter estimation. A general approach to aircraft identification adopted at NASA Langley Research Center is shown in figure 1 in the form of a block diagram. Various steps in the procedure include model postulation, design of an experiment, data compatibility analysis, model structure determination and parameter estimation combined with collinearity diagnostic, and model validation.

Model Postulation

Model postulation is influenced by the type of selected maneuver intended for system identification and by a prior knowledge about aircraft aerodynamics. The aerodynamic forces and moments are expressed in the form of polynomials or polynomial splines as

$$C_a = C_a(0) + \sum_{j=1}^{n-1} \theta_j x_j \qquad (3)$$

where C_a is the aerodynamic coefficient, $C_a(0)$ is the value of the coefficient at initial steay-state conditions and the x_j now represents input and output variables, their combinations and/or spline terms. The postulated model is then used in model structure determination and parameter estimation. For a model with unsteady aerodynamics the forces and moments can be formulated in terms of indicial functions [4,5] as

$$C_a(t) = C_a(0) + \int_0^t C_{a\xi}(t-\tau;\xi(\tau))^T \frac{d}{d\tau}\xi(\tau)d\tau \qquad (4)$$

where ξ is a vector of aircraft state and input variables upon which the coefficient C_a depends, $C_{a\xi}(t)$ is a vector of indicial functions whose elements are the responses in C_a to unit steps in ξ. The indicial responses, $C_{a\xi}$, are functions of elapsed time $(t-\tau)$ and are continuous single-valued functions of $\xi(t)$. The indicial functions approach steady-state values with increasing values of the argument $(t-\tau)$. If the indicial response $C_{a\xi}$ is only a function of elapsed time, equations (4) is simplified as

$$C_a(t) = C_a(0) + \int_0^t C_{a\xi}(t-\tau)^T \frac{d}{d\tau}\,\xi(\tau)d\tau \qquad (5)$$

When analytical forms of indicial functions are specified, the aerodynamic model based on equation (4) or (5) can be used in the aircraft equations of motion for stability and control studies involving either nonlinear or linear unsteady aerodynamics, respectively. The resulting equations of motion will be represented by a set of integro-differential equations.

Design of Experiment

The most important part of the experiment design is the selection of input forms. It has been recognized that the shape of an input signal could influence the accuracy of estimated parameters from flight measurement. Attempts for obtaining parameter estimates with high accuracy led many researchers to the development of an optimal input. One of the latest techniques for optimal input design is discussed in [6].

Data Compatibility Analysis

In practice, often the measured response data, even after careful handling, can still contain bias errors. In order to verify data accuracy, a compatibility check can be applied to the measured aircraft responses. This check includes aircraft state estimation, based on known kinematics and the available sensor measurements, estimation of unknown bias errors and a comparison of reconstructed responses with those measured. The state equations are formed by kinematic relationships and the parameter vector usually contains constant offsets and scale factor errors. The estimation techniques are similar to those used in estimation of states and aerodynamic parameters.

Methods of Parameter Estimation

Model structure determination and parameter estimation combined with collinearity diagnostic form the principal part of the identification procedure. From the postulated model and measured data the model structure can be determined as explained later. When the model structure is known the parameter estimation can follow. In aeronautical application three methods, the maximum likelihood (ML), linear regression (LR) and extended Kalman filter (EKF), are the basic techniques.

The ML estimates are obtained by maximizing the conditional probability of measurement $Z=[z(1),z(2),...,z(n)]^T$ given a value of θ, i.e.

$$\hat{\theta} = \max_{\theta} p(Z|\theta)$$

Rather than minimize $p(Z|\theta)$, it is more convenient to minimize the negative logarithm of the likelihood function $L(\theta) = p(Z|\theta)$, called log-likelihood function,

$$\hat{\theta} = \min_{\theta}\{-\ell n L(\theta)\}$$

Substantial simplification to the ML estimation is obtained by assuming no external disturbances to the system and no measurement errors in input data. Then the ML estimation is reduced to the output error method with the cost function

$$J = \frac{1}{2}\sum_{i=1}^{N} v^T(i)R^{-1}v(i) + \frac{N}{2}\ell n|R| \qquad (6)$$

where $v(i)$ are the residuals, $v(i) = z(i) - y(i,\hat{\theta})$, and R is the measurement noise covariance matrix. Experience shows that a suitable technique for minimization of (6) is the Modified Newton-Raphson method. Using this technique, the step size, $\Delta\theta$, for parameter estimates is given by

$$\Delta\hat{\theta} = M^{-1}\frac{\partial \ell n L(\theta)}{\partial\theta} \qquad (7)$$

where M is the Fisher information matrix containing products and sums of the first order partials of the log-likelihood function. The expression for the information matrix is

$$M = \sum_{i=1}^{N}\left(\frac{\partial y(i)}{\partial\theta}\right)^T R^{-1}\frac{\partial y(i)}{\partial\theta} \qquad (8)$$

The information matrix provides also a lower bound on parameter covariances, i.e.

$$Cov(\hat{\theta}) = E\{(\hat{\theta}-\theta)(\hat{\theta}-\theta)^T\} \geq M^{-1} \qquad (9)$$

The inverse of M is called the Cramer-Rao lower bound and the ML estimates approach it asymptotically as N increases. Expression (8) is valid if the measurement noise is random, Gaussian and white. Numerous analyses from measured flight data showed, however, that these residuals can be far from being white.

The residuals very often contain some deterministic components. The result is colored residuals leading to new expression for parameter covariance matrix [7] in the form

$$\mathrm{Cov}(\hat{\theta}) = M^{-1}\left[\sum_{i=1}^{N}\left(\frac{\partial y(i)}{\partial \theta}\right)^{T} R^{-1} \sum_{j=1}^{N} \Re_{vv}(i-j) R^{-1} \frac{\partial y(i)}{\partial \theta}\right] M^{-1} \quad (10)$$

where $\Re_{vv}(i-j)$ is the autocorrelation matrix for the output residual vector. It is estimated from

$$\hat{\Re}_{vv}(k) = \frac{1}{N-k} \sum_{i=1}^{N-k} v(i)\, v(i+k)^{T} = \hat{\Re}_{vv}(-k) \quad (11)$$

Further simplification to the ML method is obtained by assuming that both the input and states variables are measured without errors. This assumption leads to an equation error method which can be formulated as a linear regression applied to aerodynamic model equation (3). When the states, and inputs in this equation are replaced by measured values the equivalent of the general regression equation

$$y(i) = \theta_0 + \theta_1 x_1(i) + \ldots, \theta_{n-1} x_{n-1}(i) + \varepsilon(i) \quad (12)$$

is obtained. In this equation, y now represents a dependent variable, x_1 to x_{n-1} are the regressors and ε is the equation error. When the regression equations are expressed as

$$Y = X\theta + \varepsilon \quad (13)$$

the least squares (LS) parameter estimates are obtained as

$$\hat{\theta} = (X^{T}X)^{-1} X^{T} Y \quad (14)$$

and their covariance matrix as

$$\mathrm{Cov}(\hat{\theta}) = \sigma^{2}(X^{T}X)^{-1} \quad (15)$$

for white noise and as

$$\mathrm{Cov}(\hat{\theta}) = (X^{T}X)^{-1}\left[\sum_{i=1}^{N} x(i) \sum_{j=1}^{N} \Re_{ee}(i-j)\, x(j)^{T}\right](X^{T}X)^{-1} \quad (16)$$

for colored noise where σ^2 is the variance of $\varepsilon(i)$

$$\hat{\Re}_{ee}(k) = \frac{1}{N-K} \sum_{i=1}^{N-K} e(i)\, e(i+k) = \hat{\Re}_{ee}(-k) \quad (17)$$

and

$$e(i) = y(i) - x(i)^{T}\hat{\theta} \quad (18)$$

The linear regression is a widely used estimation method for the following reasons:

a) it is a simple non-iterative method for parameter estimation;

b) the LS estimates serve as nominal starting values for the ML and EKF methods;

c) linear regression can be applied to data generated by partitioning an ensemble of data from repeated measurements with respect to one or more variables [8];

d) linear regression can be extended to a technique for model structure determination, e.g.stepwise regression;

e) formulation of a regression problem can be used for investigation of near-linear dependence (collinearity) among measured state and input variables and for the development of biased estimation techniques for dealing with highly collinear data (see Section 3).

For the development of the EKF algorithm the state vector is augmented by a parameter vector, $x_a = [x^{T} : \theta^{T}]^{T}$. The vector x_a and its covariance matrix are estimated from measurements by minimizing the cost function

$$J = E\left\{[x_a(i|i-1) - x_a(i)]^{T}[x_a(i|i-1) - x_a(i)]\right\}$$

Because of inherent feed-back in the algorithm, the EKF can be easily applied to an unstable system for which the use of the output error method might be difficult or even impossible. On the other hand, the main disadvantage of the EKF method is that the initial conditions and the covariance matrices of process and measurement noise must be specified at the start of the estimation process.

Model Structure Determination

A major problem in system identification is the selection, from measured data, of an adequate (parsimonious) model. An adequate model is considered to be a model which sufficiently fits the data, facilitates the successful estimation of unknown parameters whose existence can be substantiated, and has good prediction capabilities. For model structure determination a method of stepwise regression is being used [9]. The determination of a model for the aerodynamic coefficients includes three steps: postulation of terms that might enter the model, selection of an adequate model, and validation of the model selected. After postulating the aerodynamic model equations, significant terms among the candidate variables are determined and the corresponding parameters estimated. At every step of the stepwise regression, the variables incorporated into the model in previous stages and a new variable entering the model are reexamined for their significance. Experience shows, however, that the model based only on the statistical significance of individual parameters in the model can still include too many terms and may have poor prediction capabilities. Several criteria for the selection of an adequate model have been,therefore, introduced. The most often used are:

a) The computed values of F-statistic, given as the ratio of regression mean square to residual mean square. Heuristically, the model with the maximum F-values is the "best" one for a given set of data.

b) The value of the coefficient of determination, R^2, which can be interpreted as measuring the proportion of the variation explained by the terms other than θ_0 in the model.

c) The prediction sum of squares PRESS defined for the k^{th} subset of model parameters as

$$\text{PRESS} = \sum_{i=1}^{N} \left(y(i) - \hat{y}[i|\,x(1),\ldots,x(i-1),x(i+1),\ldots,x(N)]_k\right)^2 \qquad (19)$$

For the model to be a good predictor the value of PRESS should be minimal.

Model Validation

Model validation is the last step in the identification process and should be applied regardless of the complexity of the estimation method. The resulting model must demonstrate that its parameters have physically reasonable values and acceptable accuracy, and that the model is a good predictor. For those reasons the parameter estimates are compared with any information available about aircraft aerodynamics. Prediction capabilities of the model are checked on a set of data not used in the identification process.

3. DATA COLLLINEARITY AND BIASED ESTIMATION

As pointed out in the Introduction the augmentation of high performance aircraft very often introduces near linear relationships among the input and output variables (data collinearity). When linear regression is used in data analysis the collinearity results in an ill-conditioned X^TX matrix in expression (14) for LS parameter estimates. Because of that the collinearity can cause computational problems and reduce the accuracy of estimates. Three procedures for detection of collinearity are recommended in [10] and applied to flight data. They are:

a) examination of the correlation matrix $X^{*T}X^{*}$ and its inverse, where the matrix X^{*} is formed by centered and scaled regressors;

b) eigenvalue analysis of the X^TX matrix or singular value decomposition of the X matrix;

c) parameter variance decomposition into a sum of components, each corresponding to one and only one of the eigenvalues of the X^TX matrix or singular values of the X matrix.

The parameter variance decomposition approach for detecting collinearity was proposed in [1]. It follows from the covariance matrix of parameter estimates $\hat{\theta}$ which can be also obtained as

$$\text{Cov}\,(\hat{\theta}) = \sigma^2 T\Lambda^{-1}T^T \qquad (20)$$

where Λ is a diagonal matrix whose elements are the eigenvalues of X^TX and T is a matrix whose columns are the eigenvectors of X^TX.

The variance of each parameter is equal to

$$\sigma^2(\hat{\theta}_j) = \sigma^2 \sum_{k=1}^{n} \frac{t_{jk}^2}{\lambda_j} = \sigma^2 \sum_{k=1}^{n} \frac{t_{jk}^2}{\mu_j^2} \qquad (21)$$

where t_{jk} are the elements of eigenvector t_j associated with λ_j. Eq. (21) decomposes the variance of each parameter into a sum of components, each corresponding to one and only one of the n singular values μ_j. In (21) the singular values appear in denominator, so one or more small singular values can substantially increase the variance of θ_j. This means that an unusually high proportion of the variance of two or more coefficients for the same small singular value can provide evidence that the corresponding near dependency is causing problems. Introducing

$$\Phi_{jk} = \frac{t_{jk}^2}{\mu_j^2} \quad \text{and} \quad \Phi_j = \sum_{k=1}^{n} \Phi_{jk}$$

the j,k variance-decomposition proportion as the

proportion of the variance of the jth regression coefficient associated with the kth components of its decomposition in (21) is given as

$$\pi_{kj} = \frac{\Phi_{jk}}{\Phi_j}, \quad j,k = 1,2,...,n \qquad (22)$$

Since two or more regressors are required to create near dependency, then two or more variances will be adversely affected by high variance-decomposition proportions associated with a single singular value. Variance-decomposition proportions greater than 0.5 are recommended in [1] as a guidance for possible collinearity problems. It is also suggested that the columns of X should be scaled to unit length but not centered. Thus the role of the bias term in near-linear dependencies can be diagnosed.

If the collinearity diagnostic reveals a serious problem some way of dealing with it should be chosen. Additional data can be selected, the experiment can be redesigned, the model can be respecified or different techniques from the ordinary LS procedure can be used. Several estimation techniques which can be applied to data with severe collinearity have been developed [11]. Their development drops the requirement that the estimator of θ be unbiased. The new estimator, however, should have smaller variance than the LS estimator. By allowing the small amount of bias the parameter variance can be made small such that the mean square error of θ is less than the variance of the unbiased LS estimator. Techniques with this property belong to a class of biased estimation methods. Two of the techniques, the mixed estimation and rank reduction regression, have been introduced in [10] and used in flight data analysis. The experience with the rank reduction regression showed some difficulties in its application to aerodynamic model equations, mainly because of small number of unknown parameters in these equations. For that reason, only the mixed estimation will be introduced.

The mixed estimation (ME) is a procedure which uses prior information on parameters to augment measured data directly instead of through a prior distribution. Mixed estimation includes the usual regression model given by eq. (13) and the additional assumption that a set of prior conditions on θ can be written as

$$d = A\theta + \zeta \qquad (23)$$

In this equation, A is a matrix of known constants and ζ is a vector of random variables with $E(\zeta) = 0$ and $E(\zeta\zeta^T) = \sigma^2 W$, where W is a known weighing matrix. Combining (13) and (23) the mixed model is obtained.

For known σ^2 the application of least squares to this model results in the mixed estimator

$$\hat{\theta}_{ME} = (X^T X + A^T W^{-1} A)^{-1} (X^T Y + A^T W^{-1} d) \qquad (24)$$

It is shown in [10] that the addition of prior information to the ordinary regression results in reduction of parameter variance. In real application of the ME the *a priori* values are not known exactly therefore the resulting estimator is biased [10].

4. EXAMPLES

In the following three examples the measured data from experiments on the X-29A, X-31A and F-16XL aircraft will be used. These examples will demonstrate mainly specific problems related to identification of high performance aircraft. In addition, variations of some parameters with the angle of attack or Mach number, and their correlation with wind tunnel data and flight results from scale model will be also shown.

4.1 X-29A Aircraft

The test vehicle is a single engine, single seat fighter-type research aircraft with forward-swept wings. The aircraft has highly relaxed static longitudinal stability in subsonic and transonic regimes and near-neutral stability in supersonic regimes. For longitudinal control, deflections of canard, wing flap (flaperon), and fuselage strake are used. The lateral control is provided by the rudder and asymmetric deflection of flaperon. In addition to manual control of the aircraft, the concept of remotely augmented vehicle (RAV) could be used for the excitation of aircraft responses. The RAV arrangement employs a ground computer to augment the onboard control system. This capability is used to introduce a command to the control stick (pitch stick or roll stick command), rudder pedal, or individual control surfaces. The RAV commands, usually a pulse or doublet, are summed onto the already existing commands in order to independently move flaps, strake, canard, rudder, or differential flap. More about the RAV system can be found in [12]. A drawing of the aircraft is presented in figure 2. A more detailed description of the aircraft and its control system is contained in [13].

The following three sets of data were available for estimation of aircraft parameters:

1. longitudinal maneuvers excited by a pilot at Mach numbers from 0.5 to 1.4,

2. longitudinal and lateral maneuvers with computer generated inputs (RAV experiment) at Mach numbers from 0.6 to 1.3,

3. low speed lateral maneuvers initiated by a pilot at the angles of attack between 8^0 to 50^0.

During data analysis several problems associated with inherent instability, high augmentation and sometimes insufficient excitation of maneuvers had to be addressed. Among them were:

1. parameter estimation of an unstable vehicle,

2. data collinearity and its diagnostics,

3. adverse effect of data collinearity on parameter identifiability and accuracy.

Because of these problems, a linear regression and mixed estimation were used in data analysis.

Time histories of a typical longitudinal pilot and computer-generated input are presented in figures 3 and 4. From figure 3 close correlation among all open-loop inputs is obvious. The change in data collinearity caused by replacing the pilot by computer-generated input as a sequence of commanded flap, strake, canard and stick deflections is demonstrated in figure 4. The collinearity was assessed by comparing correlations between regressors, and corresponding, condition indexes and parameter variance proportions. The condition index is defined as the ratio of the maximum eigenvalue of the information matrix X^TX to one of the remaining eigenvalues.

The correlation matrices for the two sets of data are given in tables I and II, respectively. The data with the pilot input show correlation between δ_c and $q\bar{c}/2V$ and δ_c and δ_s. The RAV data do not exhibit any significant correlation between regressors. The condition indexes and parameter variance proportions are given in tables III and IV. In this example the maximum condition index (condition number) for the set of data with pilot input is 174, in the second case 14, thus indicating reduced spread of eigenvalues where the RAV system was used. The variance proportions in table III for the largest condition index show strong collinearity among the bias term, canard and strake effectiveness. The same quantities in table IV indicate only a possibility of collinearity between the bias term and canard effectiveness.

Table V demonstrates a possibility of estimating parameters in the regression equation for the pitching-moment coefficient with sufficient accuracy. Included are the increments in coefficient of determination, ΔR^2, and t-statistics, t^*. The values of ΔR^2 represent the amount of information in the data explained by the individual terms in the model, t-statistic can be considered as a measure of significance of individual parameters. The data with the pilot input revealed that $C_{m\delta c}\delta_c$ is the highly influential term in the pitching-moment equation, that there is a limited possibility for accurate estimates of parameters $C_{m\delta f}$ and $C_{m\delta s}$, and that the significance of the $C_{mq}q\bar{c}/2V$ term is almost zero. The RAV experiment improved the identifiability of parameters $C_{m\alpha}$, $C_{m\delta f}$ and $C_{m\delta s}$, still maintaining the $C_{m\delta c}\delta_c$ as a dominant term. The chance for accurate estimation of C_{mq} remains small.

The estimates of two parameters $C_{m\alpha}$ and $C_{m\delta c}$ which contribute the most to the pitching moment are plotted against the Mach number in figures 5 and 6 respectively and compared with the wind tunnel results. The estimates were obtained from data with pilot input using the least squares and mixed estimation, and from RAV experiment using only the least squares method. The wind tunnel values of the strake effectiveness were used as *a priori* values. The accuracies of the *a priori* values were determined from repeated test in two different wind tunnels. As can be seen from these figures, the accuracy of parameters was improved either by applying the mixed estimation to data with pilot input or by using data from the RAV experiment. Similar conclusion can be drawn from average standard errors in estimated parameters. These values are shown in table VI together with the fit error for the coefficient C_m.

The measured data from all low speed lateral maneuvers were assembled into one set with 51,200 data points which was then partitioned into 42 one-degree-α subsets and 1 three-degree-α subset. A half of the selected lateral maneuvers was analyzed as individual maneuvers using stepwise regression. The possibility of data collinearity in measured data was investigated by procedures explained in the previous examples. Application of stepwise regression to partitioned data resulted in models for the lateral aerodynamic coefficients and least squares estimates of parameters in these models. For the data subsets with $\alpha<40^0$, models with linear stability and control derivatives were adequate. For data at $\alpha>40^0$, some nonlinear and longitudinal control terms were selected by the stepwise regression. These additional terms did not provide any comprehensive information about aerodynamic nonlinearities or effects of longitudinal control setting on the lateral aerodynamic coefficients.

The estimated parameters (stability and control derivatives) from 43 subsets were plotted against the angle of attack and fitted by quadratic polynomial splines. In addition to fitted splines, the 2σ-confidence limits on the mean were computed as

$$\hat{\theta}(\alpha) \pm 2s\sqrt{x^T(X^TX)^{-1}x} \qquad (25)$$

In (25), $\hat{\theta}$ is the mean value of a parameter given by the fitted spline, s is the standard error of $\hat{\theta}$ estimated from the residuals, x is a vector of regressors. As an example, estimated values of the parameter C_{np}, fitted spline, and 2σ-confidence limits are shown in figure 7.

Stepwise regression analysis of data from single maneuvers showed that linear models for the aerodynamic coefficients were adequate within the angle-of attack range from 8^0 to 40^0. For angles of attack greater than 40^0

models for the lateral-force and yawing-moment coefficient included some of the nonlinear terms β^2, β^3, $\alpha\beta$, $\beta\delta_e$ or δ_r^3. As for the partitioned data, there was no consistent information about parameters associated with these nonlinear terms.

The least squares parameter estimates at low and moderate angles of attack were close to results from partitioned data. For $\alpha > 20^0$, however, increased scatter in the estimates and their deviation from the previous results using partitioned data were observed. This inconsistency was caused by data collinearity detected mostly among the variables pb/2V, δ_a and δ_r. In applying the mixed estimation technique, the *a priori* values were selected for parameters which were affected by collinearity. Their changes had only a small effect on aerodynamic coefficients. The *a priori* values and their uncertainty were set to the mean values and their standard errors obtained from partitioned data. An example of data collinearity is given in table VII where the eigervalues of the information matrix, condition indexes and parameter variance decompositions are included. The damaging effect of data collinearity on parameters associated with the variables pb/2V, δ_a and δ_r can be expected. Table VIII presents the parameter estimates and their standard errors in the rolling-moment equation using stepwise regression and, mixed estimation. In the last column of table VIII the parameter estimates from partitioned data are given. Large changes in the least square estimates of $C_{\ell p}$, $C_{\ell \delta a}$ and $C_{\ell \delta r}$ are visible during the model development. The final estimates of the three parameters are also quite different from those obtained from partitioned data. On the other hand, the parameters from the mixed estimation technique are close to the result from partitioned data. These estimates also have lower standard errors than the least squares results. The decrease in the fit error, $s(C_\ell)$, and squared correlation coefficient, R^2, are not substantial (see last two rows in table VIII).

Selected parameters obtained from partitined data and single maneuvers are plotted against the angle of attack in figures 8 and 9, and compared with wind tunnel data. The 2σ - confidence limits were omitted in these figures. However, the minimum and maximum values for standard errors of the estimated parameters from partitioned data are given in table IX. Both figures indicate no significant differences between the two sets of flight results. Large differences, however exist between flight and wind tunnel results in figure 8. Flight data exhibit a sudden increase in parameter values of $C_{y\beta}$ and $C_{n\beta}$ at angles of attack around 40^0 to 45^0. As indicated by wind tunnel investigations in [14], an increase of lateral force and yawing moment due to sideslip is caused by the forebody vortex assymetry. This assymetry can produce a sideforce which moves the nose into the sideslip and thus enhances directional stability. The same effect was observed in [15] during wind tunnel testing of the scaled model. The present differences between flight and wind tunnel results can be caused by different Reynolds numbers in the two experiements (0.68×10^6 in the wind tunnel; approx. 6×10^6 during the flight test) and by the effect of the nose boom on the full scale aircraft. Positive yaw damping for $\alpha > 30^0$ is predicted by flight data whereas the wind tunnel results show low yaw damping over the whole range of angles of attack. In figure 9 three rolling moment parameters are included. The parameter $C_{\ell\beta}$ estimated from flight data agrees, in general, with wind tunnel predicitions. The roll damping decreases above $\alpha = 15^0$, from wind tunnel above $\alpha = 25^0$. Positive values of $C_{\ell p}$ from flight are about three times higher than those from wind tunnel. As mentioned in [15] and [16] the forebody aerodynamics dominates the roll-damping parameter at high angles of attack and causes the unstable damping. Therefore the differences between flight and wind tunnel results maybe attributed to different forebody aerodynamics in these two test conditions. The parameter $C_{\ell\delta a}$ is estimated with high consistency and agrees well with wind tunnel data for the angles of attack between 12^0 and 40^0. Some differences exists outside this interval. More about the parameters can be found in [17].

The results from this example lead to the following conclusions:

1. A collinearity diagnostic and a comparison of parameter estimates from flight data using the RAV experiment with those from flight data using pilot input revealed that the computer-generated deflections of individual control surfaces can substantially decrease data collinearity. A simple least squares technique can be used in estimation of all parameters in the model which also means estimation of the effectiveness of all controls used.

2. The experiment providing the data for the analysis was not properly designed. The selected input forms resulted in very small excitation of response variables. As a result some parameters were not identifiable and the identifiability of several remaining parameters was significantly reduced. These identifiability problems were apparent from the diagnostic of selected maneuvers.

3. For low speed lateral maneuvers linear aerodynamic models determined by applying stepwise regression techniques to partitioned data and single maneuvers were found to be adequate for the angles of attack less than 40^0. For angles of attack greater than 40^0, nonlinear and longitudinal control terms entered the models selected by the estimation technique. These terms, however, did not provide any comprehensive information about aerodynamic nonlinearities and the effect of longitudinal control on lateral aerodynamic coefficients. Because of data collinearity detected in single maneuvers, the data from these maneuvers were reanalyzed by using mixed estimation. No significant differences existed between parameters estimated from partitioned data and those estimated from single maneuvers.

4.2. X-31A Aircraft

The X-31A is a single engine, single seat fighter-type research aircraft with delta wing and canard. The aircraft is inherently unstable in subsonic regimes and is controllable by a digital control system. For longitudinal

control, canard and symmetrical flaperon deflections are used. The lateral control is provided by the rudder and differential flaperon. In addition to the aerodynamic control surfaces, a three-vane thrust vectoring system is mounted around the engine exhaust nozzle. This system allows thrust deflection up to 15^0 and is used for augmentation of pitch and yaw control during low speed and post-stall flights. A drawing of the aircraft is presented in figure 10.

Maneuvers from eight flights were selected for aerodynamic model structure determination and parameter estimation. These maneuvers were initiated from trim conditions at altitudes between 6,000 to 9,000 meters and angles of attack between 10^0 and 70^0. Two types of input were used, the pilot inputs and inputs generated by a flutter test box installed on one of the aircraft. The pilot inputs were either pitch command or yaw and roll commands in the form of a single doublet or a combination of doublets. The flutter test box allowed separate excitation of all aerodynamic control surfaces. These inputs were in the form of "3211" multiple signals. The surface deflection limits in the tests were 7.1^0 for the canard, 11.8^0 for the flaperons and 7.8^0 for the rudder. To ensure good excitation of aircraft motion, the longitudinal inputs were in some cases preceded by the pilot pitch doublets and the lateral inputs by pilot roll and yaw doublets. Maneuvers with pilot inputs were flown with thrust vectoring off ($\alpha<30^0$) and on. The single surface excitation maneuvers were realized only with thrust vectoring on.

Estimated parameters from flight data were correlated with those obtained from wind tunnel data and drop model experiment. Static and dynamic wind-tunnel test were conducted at the 30 - by 60 - Foot Tunnel at NASA LaRC using a 19 - percent scale model (see [18] for some results). For a comparison with flight results presented, the parameters C_{ℓ_p} and C_{ℓ_r} were estimated from the oscillatory data using the techniques of [19] and [3]. More about this analysis will be presented in the third example.

In preparation for X-31A flight testing, the unpowered, 27-percent dynamically-scaled radio-controlled model of the X-31A was built and tested at NASA LaRC. During the test, the model was attached to a helicopter and lifted to an altitude between 1,500 and 3,000 m, and then released with the helicopter in forward motion. At an altitude of about 300 m the flight was terminated by deploying a large parachute. The model was controlled by a pilot on the ground but the model also had the capability to accept preprogrammed surface deflection commands. This feature was used in generating maneuvers for the purpose of parameter estimation. During the experiment, only the lateral parameters were estimated. They are presented in [20]. In this paper only estimates of four lateral parameters and two thrust vectoring parameters are presented. More results can be found in [21].

Lateral parameters:

In maneuvers with pilot inputs, high augmentation prevented sufficient excitation of sideslip angle and lateral acceleration, especially at angles of attack above 30^0, and introduced high pairwise correlation between variables p and r, δ_a and δ_r, δ_r and δ_{qtv}. The effect of limited excitation and high correlation was reflected in low accuracy of parameter estimates and, in many cases, inability to estimate some parameters at all. In the rolling-moment equation the terms with δ_a and β were predominant, explaining about 75% variation in the data of the 87% for the complete model. The main influential terms in the yawing-moment equation were those with either δ_r (for low α) or δ_{qtv} in maneuvers at high angles of attack. Their contribution represented about 85 to 96% from the overall value of 98% for the model with all terms included.

The parameter identifiability was improved, in general, by the introduction of a single surface excitation (δ_a or δ_r inputs). The above mentioned correlations were substantially reduced and the amplitude of sideslip angle increased. As a result of that, parameter identifiability in the rolling-moment equation was improved. However, the problem of accurate parameter estimation in the yawing-moment and lateral-force equations remained, with the exception of the thrust-vectoring effectiveness. Four parameters in the rolling-moment equation

$$C_\ell = C_{\ell_o} + C_{\ell_\beta}\beta + C_{\ell_p}\frac{pb}{2V} + C_{\ell_r}\frac{rb}{2V} + C_{\ell_{\delta a}}\delta_a + C_{\ell_{\delta r}}\delta_r \qquad (26)$$

are presented in figure 11 with their 2σ-error bounds. In this figure the results from wind tunnel and drop model tests are also included. The estimates of C_{ℓ_β} are consistent with the exception of the region around $\alpha=25^0$. There is significant departure of flight results from wind tunnel data for the angle of attack between 30 and 45^0. The reason for that has not been explained yet. Small scatter is also apparent in the estimates of $C_{\ell_{\delta a}}$. The flight data demonstrate about 50% reduction in aileron effectiveness when compared to wind tunnel values. The estimates of C_{ℓ_p} and C_{ℓ_r} demonstrate the advantage of single surface excitation over pilot induced maneuvers. In the latter case, high correlation between rolling and yawing velocities, and low information content in the data prevented the estimates of both oscillatory parameters. There are no substantial differences between full-scale flight and wind tunnel estimates of these two dynamic parameters. The drop model parameter values at $30^0<\alpha<45^0$ are scattered with values lower than indicated by results from full-scale aircraft test.

Thrust vectoring effectiveness:

The parameter $C_{m\delta qtv}$ was estimated directly from

maneuvers with the δ_c inputs because the adequate model for the pitching moment included only variable α, δ_e and δ_{qtv}. These three regressors were not correlated. The maneuvers with δ_c inputs provided estimates of $C^*_{m\delta e}$ for $\alpha<45^0$ and $C^*_{m\delta qtv}$ for $\alpha>45^0$. From these estimates the thrust vectoring effectiveness was computed as

$$C_{m\delta qtv} = \left(C^*_{m\delta e} - C_{m\delta e}\right)\frac{\delta_e}{\delta_{qtv}}$$

or

$$C_{m\delta qtv} = C^*_{m\delta qtv} - C_{m\delta e}\frac{\delta_e}{\delta_{qtv}} \qquad (27)$$

where the relation δ_c / δ_{qtv} was evaluated from measured data and where the values of $C_{m\delta e}$ were obtained from maneuvers with pilot input (no thrust vectoring) and δ_c input. The values of the thrust-vectoring effectiveness, $C_{n\delta rtv}$, were estimated from the data with pilot input and single surface excitation. In the first cases, only maneuvers for $\alpha>35^0$ were used because the effect of rudder deflection on the yawing moment was small. When necessary the final estimates were corrected for the effect of the rudder deflection by computing $C_{n\delta rtv}$ from the estimated values of $C^*_{n\delta rtv}$ as

$$C_{n\delta rtv} = C^*_{n\delta rtv} - \frac{\delta_r}{\delta_{rtv}}C_{n\delta r} \qquad (28)$$

From maneuvers excited by a single surface deflection, the parameter $C_{n\delta rtv}$ was estimated directly. Both parameters $C_{m\delta qtv}$ and $C_{n\delta rtv}$ are plotted against the thrust coefficient in figure 12 and compared with their theoretical values

$$C_{m\delta qtv} = -\frac{x_{tv}}{\bar{c}}C_T$$
$$C_{n\delta rtv} = -\frac{x_{tv}}{b}C_T \qquad (29)$$

where x_{tv} is the distance of thrust impact point from airplane center of gravity. So far there has been no explanation for the differences between the theory and the experiment.

From the results presented here and in [22] the following conclusions can be drawn:

1. In piloted maneuvers, high correlations between input and output variables were observed. These correlations resulted in low accuracy of estimated parameters and prevented estimation of effectiveness of several control surfaces.

2. Single surface excitation reduced the above mentioned correlations. It was possible to estimate the effectiveness of all controls and increase the accuracy of estimated parameters.

3. The accuracy of parameters was also affected by their low sensitivity and small excitation of response variables, especially at high angles of attack.

4. All the influential parameters were, in general, in agreement with wind tunnel data and results from drop model tests. Some unexplained differences were, however, observed.

5. The estimated thrust vectoring effectiveness was found lower than its theoretical values.

6. The predictive capabilities of the resulting model determined from flight test data are very good for low amplitude maneuver at low to moderate angles of attack. Some deterioration in prediction was observed at high angles of attack.

4.3. F-16XL Aircraft

For better understanding of aircraft aerodynamics in large amplitude maneuvers, NASA LaRC conducted a series of wind tunnel tests on a model of the F-16XL. A sketch of the 0.10 - scale model is shown in figure 13 together with some basic model dimensions. Tests included measurement of aerodynamic forces and moments under static conditions, followed by oscillatory test about all three body axes and ramp tests in pitch. One of the reasons for the testing was to determine a mathematical model with unsteady aerodynamic terms from oscillatory data at different angles of attack and frequencies. In this paper only limited results from small amplitude ($\pm 5^0$) oscillations in pitch will be shown. More results can be found in [3] and upcoming reports.

For the following analysis of the oscillatory data it is assumed that the aerodynamic coefficients are linear functions of the angle of attack, pitching velocity and their rates. Then, for example, the increment in the lift coefficient with respect to its mean value can be formulated as

$$\Delta C_L = C_{L\alpha}\Delta\alpha + \frac{\ell}{V}C_{L\dot{\alpha}}\dot{\alpha} + \frac{\ell}{V}C_{Lq}q + \left(\frac{\ell}{V}\right)^2 C_{L\dot{q}}\dot{q} \qquad (30)$$

then for the harmonic motion

$$\Delta C_L = \alpha_A\left(C_{L\alpha} - k^2 C_{L\dot{q}}\right)\sin\omega t + \alpha_A k\left(C_{L\dot{\alpha}} + C_{Lq}\right)\cos\omega t$$
$$= \alpha_A\left(\bar{C}_{L\alpha}\sin\omega t + k\bar{C}_{Lq}\cos\omega t\right) \qquad (31)$$

where α_A is the amplitude, ω the angular frequency and

$$\alpha_A\bar{C}_{L\alpha} = \alpha_A\left(C_{L\alpha} - k^2 C_{L\dot{q}}\right)$$

$$\alpha_A k\bar{C}_{Lq} = \alpha_A k\left(C_{L\dot{\alpha}} + C_{Lq}\right)$$

represent the Fourier coefficients. The in-phase and out-of-phase components of C_L ($\bar{C}_{L_\alpha}$ and $\bar{C}_{L_q}$) can be obtained by integrating the time histories of ΔC_L over a selected number of cycles. The in-phase and out-of-phase components of C_L are plotted against the angle of attack in figure 14. The figure shows the effect of frequency which is especially strong on the out-of-phase components. A comparison of steady and oscillatory data is given in figure 15.

A strong dependence of wind tunnel oscillatory data on frequency lead to the development of models with unsteady aerodynamic terms, see e.g. [20] and [3]. As an example, the model for the lift increment was formulated in [20] as

$$\Delta C_L = \int_0^t C_{L\alpha}(t-\tau)\frac{d}{d\tau}\alpha\, d\tau + \frac{\ell}{V}\int_0^t C_{Lq}(t-\tau)\frac{d}{d\tau}q(\tau)d\tau \qquad (32)$$

where $C_{L\alpha}(t)$ and $C_{Lq}(t)$ are the indicial functions.

For obtaining the model with limited number of parameters, it was assumed that the effect of $\dot{q}(t)$ on the lift could be neglected and the indicial function $C_{L\alpha}(t)$ can be expressed as

$$C_{L\alpha}(t) = a(1-e^{-b_1 t}) + c \qquad (33)$$

Considering the above mentioned assumptions, equation (33) is simplified as

$$\Delta C_L = C_{L\alpha}(\infty)\alpha(t) - a\int_0^t e^{-b_1(t-\tau)}\frac{d}{d\tau}\alpha(\tau)d\tau + \frac{\ell}{V}C_{Lq}(\infty)q(t) \qquad (34)$$

where $C_{L\alpha}(\infty)$ and $C_{Lq}(\infty)$ are the rates of change of C_L with α and q in steady flow. The steady form of equation (32) for harmonic changes in α is identical to that of equation (31), that is

$$\Delta C_L(t) = \alpha_A \bar{C}_{L\alpha}\sin\omega t + \alpha_A k\bar{C}_{Lq}\cos\omega t \qquad (35)$$

However, with the indicial function of equation (33), the expressions for $\bar{C}_{L\alpha}$ and $\bar{C}_{Lq}$ have the form

$$\bar{C}_{L\alpha} = C_{L\alpha}(\infty) - a\frac{\tau_1^2 k^2}{1+\tau_1^2 k^2} \qquad (36)$$

$$\bar{C}_{Lq} = C_{Lq}(\infty) - a\frac{\tau_1}{1+\tau_1^2 k^2} \qquad (37)$$

where $\tau_1 = V/b_1\ell$ is the nondimensional time constant.

From the experiment, the in-phase and out-of phase components are usually obtained for different values of the angle of attack and reduced frequency while keeping the amplitude of the oscillations constant. Then the equations (36) and (37) can be generalized as

$$\bar{u}_{ji} = u_i - a_i z_{uj} \qquad (38)$$

$$\bar{v}_{ji} = v_i - a_i z_{vj} \qquad (39)$$

These equation define Model I where for the lift coefficient

$$u_i = C_{L\alpha}(\alpha_i) \qquad v_i = C_{Lq}(\alpha_i)$$

$$z_{uj} = \frac{\tau_1^2 k_j^2}{1+\tau_1^2 k_j^2} \qquad z_{vj} = \frac{\tau_1}{1+\tau_1^2 k_j^2}$$

for $i = 1,2,\ldots,n$ and $j = 1,2,\ldots,m$

In equations (38) and (39) there are, in general, $3n+1$ unknown parameters: u_i, v_i, a_i and τ_1. They can be estimated from experimental data $\bar{u}_{ji}$ and $\bar{v}_{ji}$ by minimizing the cost function

$$J_I = \sum_{j=1}^{m}\sum_{i=1}^{n}\left\{\left[\bar{u}_{ji} - (u_i - a_i z_{uj})\right]^2\right\} + \left\{\left[\bar{v}_{ji} - (v_i - a_i z_{vj})\right]^2\right\}$$

In formulating airplane equations of motion it might be more convenient to obtain expressions for u, v, and a as a function of the angle of attack rather than their discrete values. For that reason the previous model was reformulated as Model II defined by the following equations:

$$\bar{u}_{ji} = u(\alpha_i) - a(\alpha_i) z_{uj} \qquad (40)$$

$$\bar{v}_{ji} = v(\alpha_i) - a(\alpha_i) z_{vj} \qquad (41)$$

The form of expressions for $u(\alpha_i)$, $v(\alpha_i)$ and $a(\alpha_i)$ can be either specified from the variation of estimated parameters in Model I or the form can be postulated in terms of polynomials and/or polynomial splines. In the second case adequate models for $u(\alpha)$, $v(\alpha)$ and $a(\alpha)$ can be determined from measured data by a stepwise regression. The previously estimated value of parameter τ_1 can be used as an *a priori* value thus simplifying the parameter estimation procedure using Model II and the cost function

$$J_{II} = \sum_{j=1}^{m}\sum_{i=1}^{n}\left\{\left[\bar{u}_{ji} - (u(\alpha_i) - a(\alpha_i) z_{uj})\right]^2 + \left[\bar{v}_{ji} - (v(\alpha_i) - a(\alpha_i) z_{vj})\right]^2\right\}$$

Both estimation procedures were applied to oscillatory

data at four frequencies. The data for frequency k = 0.19 were used to demonstrate model prediction capabilities. The parameters $C_{L_\alpha}(\infty)$, $C_{L_q}(\infty)$ and a in both models are plotted in figure 16. The agreement between both sets of results is very good. The parameter $C_{L_\alpha}(\infty)$ agree well with that from static data. Low accuracy in $C_{L_q}(\infty)$ could result from small number of data points and small sensitivity of this parameter. The parameter a indicated smooth variation of unsteady term with the angle of attack and the largest effect of unsteady terms on the coefficient at α around 40^0. The estimated value of τ_1 was 17.2 ± 1.0, which means $b_1 = 2.71 \pm 0.16$(sec). This result indicates that the time constant associated with the unsteady effect is about 0.4 sec. The predicted components from model eq.(40) and (41) for k = 0.19 are presented in figure 17 together with the corresponding measured values. This figure demonstrates that Model II is a good predictor. Similar result was obtained for Model I.

As follows from this example, a strong dependence of wind tunnel oscillatory data on frequency led to the development of model with unsteady aerodynamic terms in the form of indicial functions. These functions were postulated as simple exponentials where the unknown parameters included aerodynamic derivatives, the exponent and multiplication term.

5. CONCLUDING REMARKS

System identification applied to aircraft has proven to be a powerful tool for aircraft modeling based on experimental data. In recent years the introduction of highly maneuverable, inherently unstable and highly augmented aircraft has required high sophistication in aircraft identification methodology. At present this methodology includes basic steps: model postulation, experiment design, data compatibility analysis, model structure determination and parameter estimation combined with collinearity and identifiability diagnostics, and model validation.

The examples presented demonstrated the need for the introduction of an on-board computer generated input signals. This system and the optimal input design procedure improve identifiability of aerodynamic models and accuracy of estimated parameters. The various modifications of the ordinary least square method proved to be basic tools for model structure determination, parameter estimation and data collinearity assessment. The resulting parameters can be used as nominal values in the application of two parameter estimation techniques used in aircraft application, the maximum likelihood method (usually in the form of output error method) and the extended Kalman filter method. For meaningful information about the identified model, the parameter estimates should be completed by their covariances thus indicating the accuracy of parameters and their correlation.

In many applications of system identification methodology, only data from small excursions from trim conditions were available. By repeating the identification using data at different trim conditions, an extended model could be constructed. However, for obtaining a global model from flight data a dedicated experiment would be needed. In this experiment modeling and optimal input design would play the major role. One of the possibilities for an extension of traditional aerodynamic model is the inclusion of unsteady effects. Some initial work has already been done mostly using data from dynamic wind tunnel testing. A strong dependency of oscillatory data on frequency led to identified models with time varying terms in the form of indicial functions. Based on these experiences the extension to flight data will follow.

References

1. Belsley, D.A.; Kuh E. and Welsh, R.E.: "Regression Diagnostics: Identifying Influential Data and Sources of Collinearity", John Wiley & Sons, Inc., 1980.

2. Goman, M. and Khrabrov, A.: "State-Space Representation of Aerodynamic Characteristics of an Aircraft at High Angles of Attack", Journal of Aircraft, Vol. 31, No. 5, 1994.

3. Klein, Vladislav; Murphy, Patrick C.: Curry, Timothy J. and Brandon, Jay M.: "Analysis of Wind Tunnel Longitudinal Static and Oscillatory Data of the F-16XL Aircraft", NASA/TM-97-206276, 1997.

4. Tobak, Murray and Shiff, Lewis B.: "On the Formulation of the Aerodynamic Characteristics in Aircraft Dynamics", NASA TR R-456, 1976.

5. Klein, Vladislav and Noderer, Keith D.: "Modeling of Aircraft Unsteady Aerodynamic Characteristics. Part 1-Postulated Models", NASA TM 109120, 1994.

6. Morelli, Eugene A.: "Advances in Experiment Design for High Performance Aircraft", in "System Identification for Integrated Aircraft Development and Flight Testing", in RTA Conference Proceedings, Paper No. 8, 5-7, Madrid, Spain, May, 1998.

7. Morelli, E. A. and Klein, V.: "Accuracy of Aerodynamic Model Parameters Estimated From Flight Test Data", Journal Guidance, Control and Dynamics, Vol. 20, No. 1, 1997, pp. 74-80.

8. Batterson, J. G. and Klein, V.: "Partitioning of Flight Test Data for Aerodynamic Modeling of Aircraft at High Angles of Attack", Journal of Aircraft, Vol. 26, No. 4, 1987, pp. 334-339.

9. Klein, V.: Batterson, J. G. and Murphy, P. C.: "Determination of Airplane Model Structure From Flight Data by Using Modified Stepwise Regression", NASA TP-1916, 1981.

10. Klein, V.: "Two Biased Estimation Techniques in Linear Regression. Application to Aircraft", NASA TM-100570, 1988.

11. Hocking, R. R.; Speed, M. D. and Lynn, M. J.: "A Class of Biased Estimators in Linear Regression", Technometrcs, Vol. 18, No. 4, Nov. 1976, pp. 425-437.

12. Mackal, D. A.; Picket, M. D.; Shilling, L. J. and Wagner, C. A.: "The NASA Integrated Test Facility and its Impact on Flight Research", AIAA Paper No. 88-2095, 1988.

13. Gera, Joseph: "Dynamic and Controls Flight Testing of the X-29A Airplane", NASA TM-86803, 1986.

14. Brandon, J. M. and Nguyen, L.T.: "Experimental Study of Effects of Forebody Geometry on High Angle of Attack Static and Dynamic Stability", AIAA Paper No. 86-0331, 1986.

15. Murri, Daniel G.; Nguyen, Luat T. and Grafton, Sue B.: "Wind-Tunnel Free-Flight Investigation of A Model of a Forward-Swept-Wing Fighter Configuration", NASA TP-2230, 1984.

16. Grafton, Sue B.; Chambers, Joseph R. and Coe, Paul L. Jr.: "Wind-Tunnel Free-Flight Investigation of a Model of a Spin-Resistant Fighter Configuration", NASA TN D-7716, 1974.

17. Klein, Vladislav; Cobley, Brent R. and Noderer, Keith D.; "Lateral Aerodynamic Parameters of the X-29 Aircraft Estimated From Flight Data at Moderate to High Angles of Attack", NASA TM-104155, 1991.

18. Croom, M. A.; Fratelo, D. J.; O'Rourke, M. J. and Trilling, T. W.: "Dynamic Model Testing of the X-31A Configuration for High-Angle-of Attack Flight Dynamic Research", AIAA Paper 93-3674-CP, 1992.

19. Klein, Vladislav and Noderer, Keith D.: "Modeling of Aircraft Unsteady Aerodynamic Characteristics. Part 2-Parameters Estimated From Wind Tunnel Data", NASA TM-11016661, 1995.16

20. Klein, V. and Noderer, K. D.: "Aerodynamic Parameters of the X-31 Drop Model Estimated From Flight Data at High Angles of Attack", AIAA Paper 92-4357-CP, 1992.

21. Klein, Vladislav and Nguyen, Luong V.: "Aerodynamic and Thrust Vectoring Parameters of the X-31A Aircraft Estimated From Flight Data at Moderate to High Angles of Attack", in "High-Angle-of Attack Technology Conference", NASA Langley Research Center, September 17-19, 1996, Hampton, VA.

Table I. X^TX matrix in correlation form. Pilot input.

α	$\frac{q\bar{c}}{2V}$	δ_s	δ_r	δ_c
1.000	0.151	0.753	0.711	-0.795
	1.000	0.318	-0.341	-0.979
		1.000	0.643	-0.928
			1.000	-0.844
				1.000

Table II. X^TX matrix in correlation form. RAV experiment.

α	$\frac{q\bar{c}}{2V}$	δ_s	δ_r	δ_c
1.000	0.275	0.673	0.328	-0.772
	1.000	0.345	-0.375	-0.089
		1.000	0.098	-0.578
			1.000	-0.303
				1.000

Table III. Collinearity diagnostic. Pilot input.

Eigenvalue	Condition index	Variance proportions (scaled regressors)					
		1	α	$\frac{q\bar{c}}{2V}$	δ_s	δ_f	δ_c
3.3102	1	0.0000	0.0092	0.4806	0.0017	0.0006	0.0001
1.2781	3	0.0099	0.0001	0.0397	0.0720	0.0058	0.0001
1.0333	3	0.0001	0.2572	0.1604	0.0000	0.0342	0.0002
0.2613	13	0.0504	0.1140	0.0991	0.0762	0.1887	0.0245
0.0981	34	0.1220	0.6194	0.2143	0.0041	0.7123	0.0548
0.0190	174	0.8176	0.0001	0.0061	0.8460	0.0585	0.9204

Table IV. Collinearity diagnostic for RAV experiment.

Eigenvalue	Condition index	Variance proportions (scaled regressors)					
		1	α	$\frac{q\bar{c}}{2V}$	δ_s	δ_f	δ_c
2.5320	1	0.0003	0.0017	0.8594	0.0003	0.0000	0.0018
1.4339	2	0.0905	0.0002	0.0049	0.0008	0.0132	0.1901
1.0028	3	0.0156	0.2543	0.0098	0.1481	0.1685	0.2565
0.4745	5	0.2173	0.0355	0.0171	0.0178	0.4886	0.0172
0.3798	7	0.0460	0.6463	0.0220	0.4605	0.0094	0.0506
0.1771	14	0.6302	0.0621	0.0867	0.3724	0.4720	0.7147

Table V. Identifiability diagnostic.

Parameter	RAV		Pilot input	
	ΔR^2, %	|t*|	ΔR^2, %	|t*|
C_{m_α}	9.09	64.8	5.06	28.0
C_{m_q}	1.08	13.7	0.01	0.0
$C_{m_{\delta_c}}$	75.74	99.1	91.49	12.3
$C_{m_{\delta_f}}$	18.35	46.4	0.94	9.2
$C_{m_{\delta_s}}$	4.46	42.7	1.00	9.2

Table VI. Average standard errors of estimated parameters.

Parameter	RAV	Pilot input	
	LS	LS	ME
$s(C_{m_\alpha})$	0.029 (0.014)	0.058 (0.075)	0.054 (0.020)
$s(C_{m_{\delta_c}})$	0.017 (0.018	0.090 (0.037)	0.048 (0.020)
$s(C_m)$	0.0033 (0.0011)	0.0059 (0.0026)	0.0060 (0.0026)

Note: figures in parentheses are standard errors.

Table VII. Collinearity diagnostic.

Eigenvalue	Condition index	Variance proportions (scaled and centered regressors)				
		β	$\frac{pb}{2V}$	$\frac{rb}{2V}$	δ_a	δ_r
2.387	1.0	0.000	0.005	0.002	0.013	0.007
1.849	1.3	0.085	0.000	0.084	0.006	0.004
0.537	4.4	0.167	0.001	0.528	0.022	0.001
0.209	11.4	0.540	0.000	0.002	0.207	0.079
0.017	140.4	0.208	0.994	0.384	0.752	0.910

Table VIII. Identifiability diagnostic and parameter estimates.

Parameter	Stepwise Regression					Mixed* estimation	Partitioned data
	n = 2	n = 3	n = 4	n = 5	n = 6		
C_{l_0}	-0.0036	-0.0014	-0.0028	-0.0031	-0.0020	-0.0172	-
C_{l_β}	-0.272 (0.0080)	-0.246 (0.0072)	-0.221 (0.0070)	-0.223 (0.0064)	-0.190 (0.0057)	-0.208 (0.0056)	-0.254 (0.0087)
C_{l_p}	-	-	0.3 (0.15)	1.4 (0.13)	2.3 (0.12)	0.84 (0.050)	0.62 (0.046)
C_{l_r}	-	-	-	-	-3.3 (0.26)	-1.2 (0.22)	-1.04 (0.095)
$C_{l_{\delta_a}}$	-	0.028 (0.0058)	0.049 (0.0055)	0.081 (0.0050)	0.106 (0.0046)	0.064 (0.0035)	0.064 (0.0041)
$C_{l_{\delta_r}}$	-	-	-	0.031 (0.0053)	0.054 (0.0047)	0.015 (0.0010)	0.01 (0.0021)
s(C$_l$)	0.0050	0.0045	0.0043	0.0040	0.0035	0.0040	-
R^2[%]	83.4	86.8	87.6	89.7	91.7	88.0	-

* a priori value $C_{l_{\delta_r}} = 0.010 \pm 0.0021$

Note: figures in parentheses are standard errors

Table IX. Standard errors of estimated parameters from partitioned data.

Parameter	Standard Error	
	min	max
C_{Y_β}	0.045	0.15
C_{Y_p}	0.42	1.1
C_{Y_r}	0.78	2.3
$C_{Y_{\delta_a}}$	0.026	0.060
$C_{Y_{\delta_r}}$	0.016	0.053
C_{l_β}	0.0076	0.016
C_{l_p}	0.040	0.11
C_{l_r}	0.063	0.18
$C_{l_{\delta_a}}$	0.0037	0.011
$C_{l_{\delta_r}}$	0.0021	0.0044
C_{n_β}	0.0064	0.020
C_{n_p}	0.054	0.12
C_{n_r}	0.086	0.31
$C_{n_{\delta_a}}$	0.0029	0.0070
$C_{n_{\delta_r}}$	0.0013	0.0051

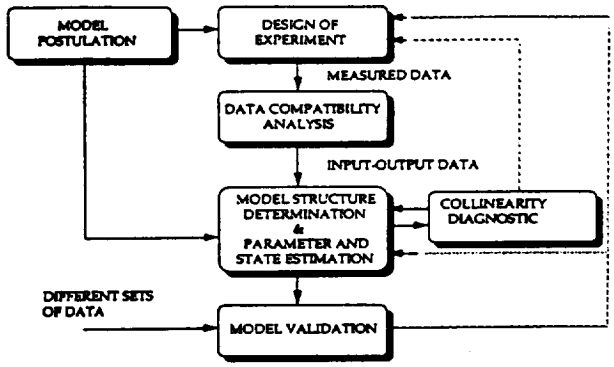

Figure 1. Block diagram of aircraft identification.

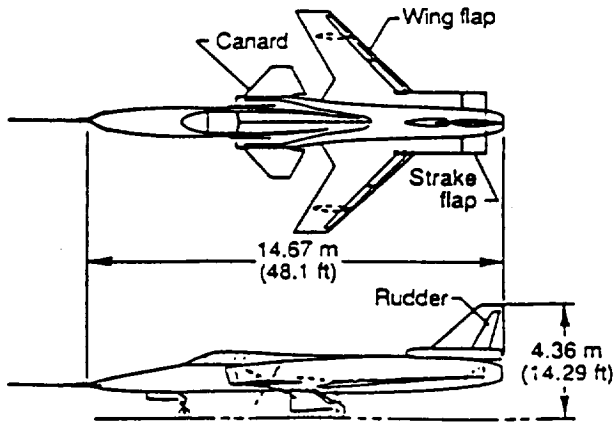

Figure 2. Drawing of X-29A aircraft.

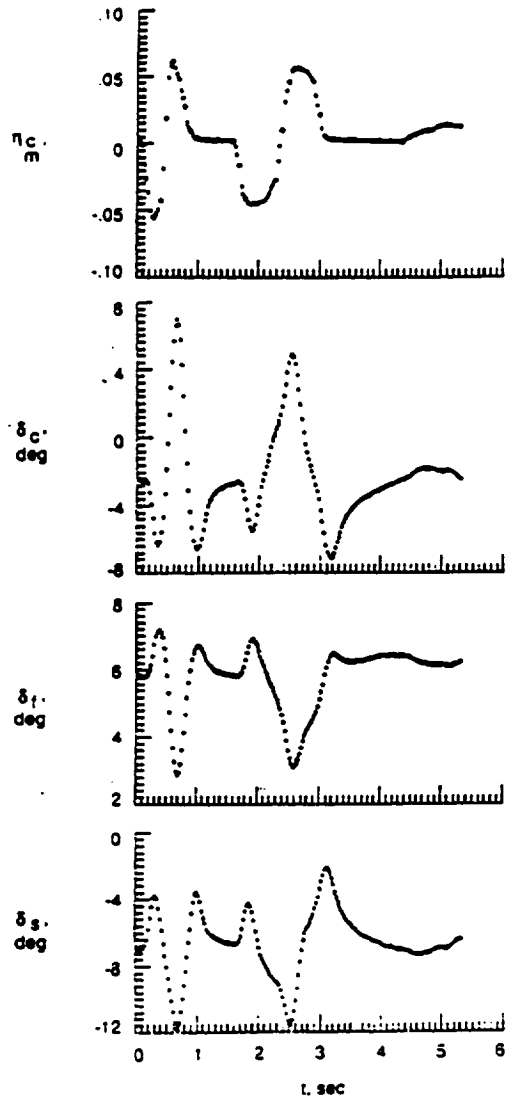

Figure 3. Time histories of measured input variables. Pilot input.

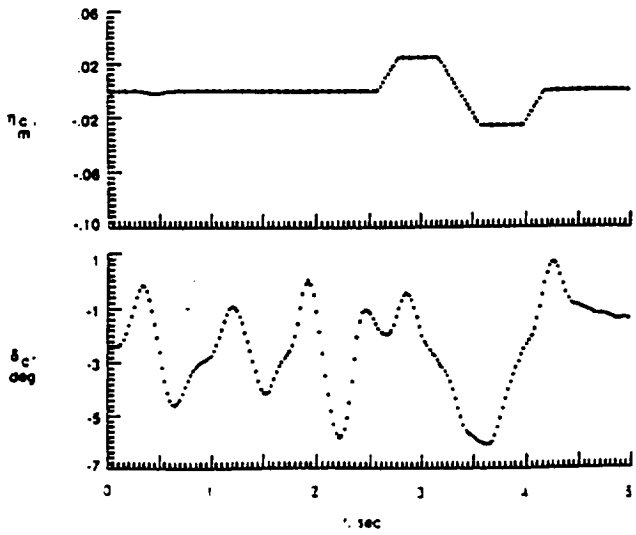

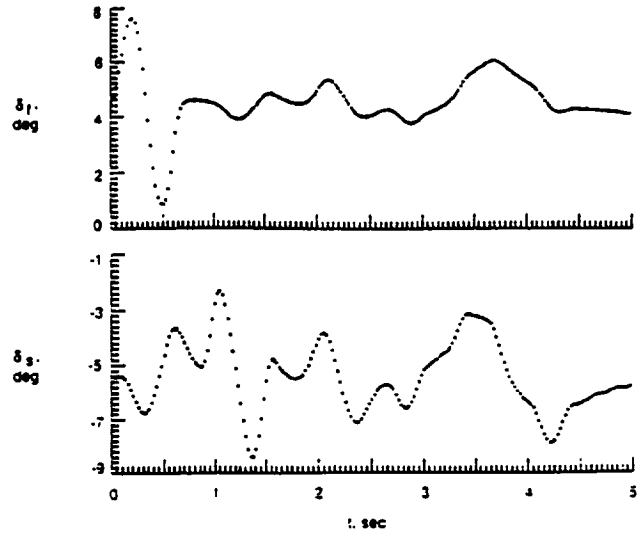

Figure 4. Time histories of measured input variables. RAV experiment.

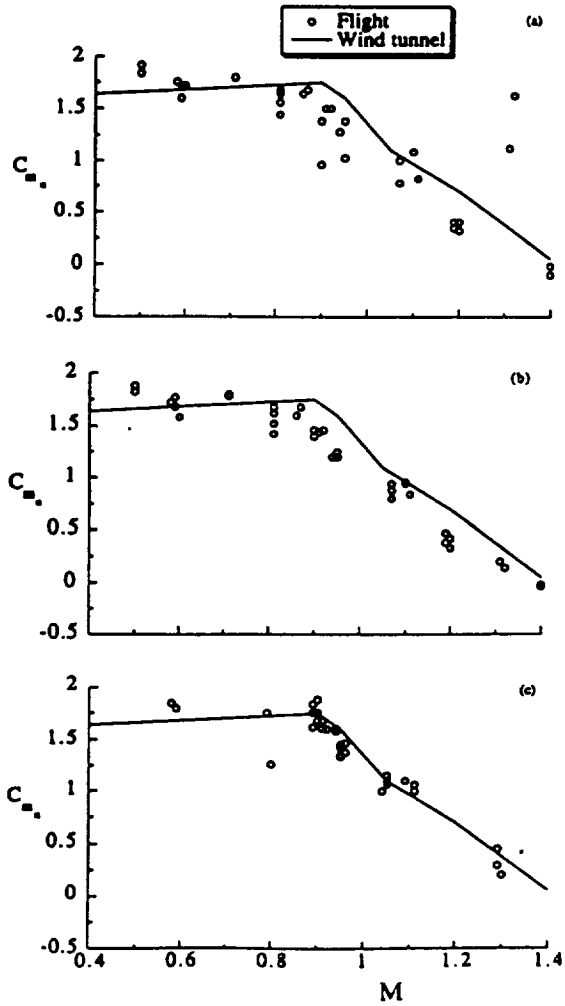

Figyre 5. Static-stability parametr estimated from flight data with pilot input by using (a) least squares, (b) mixed estimation, (c) from RAV experiment.

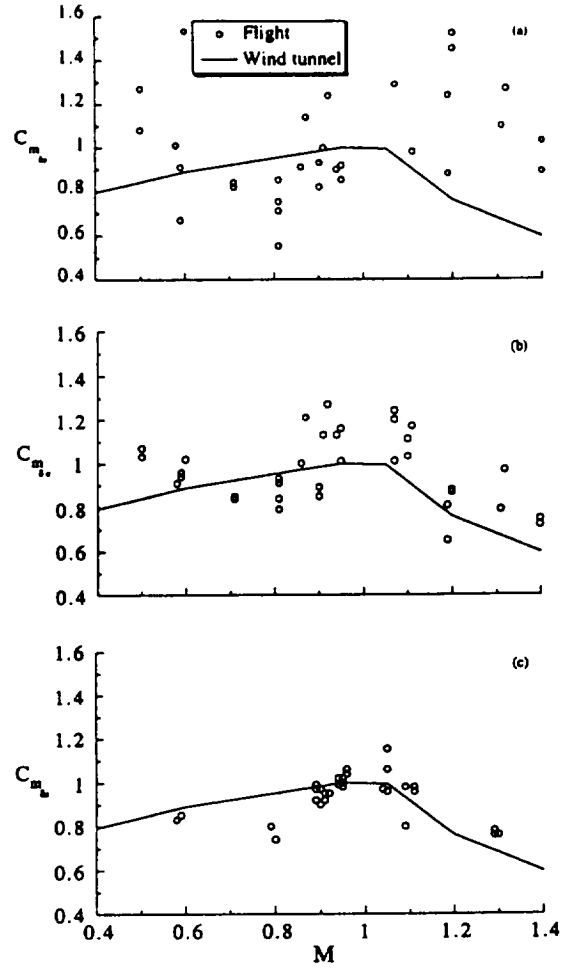

Figure 6. Canard effectiveness estimated from flight data with pilot input by using (a) least squares, (b) mixed estimation, (c) from RAV experiment.

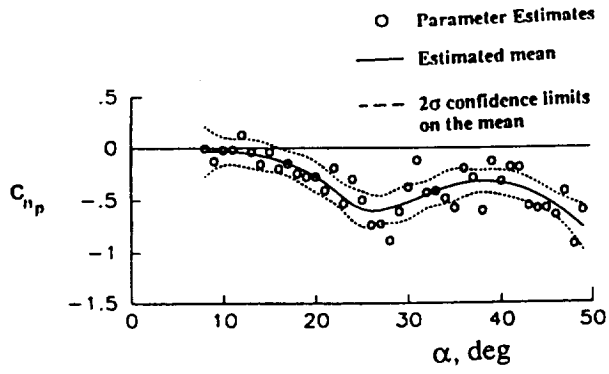

Figure 7. Roll-rate parameter estimated from partitioned data.

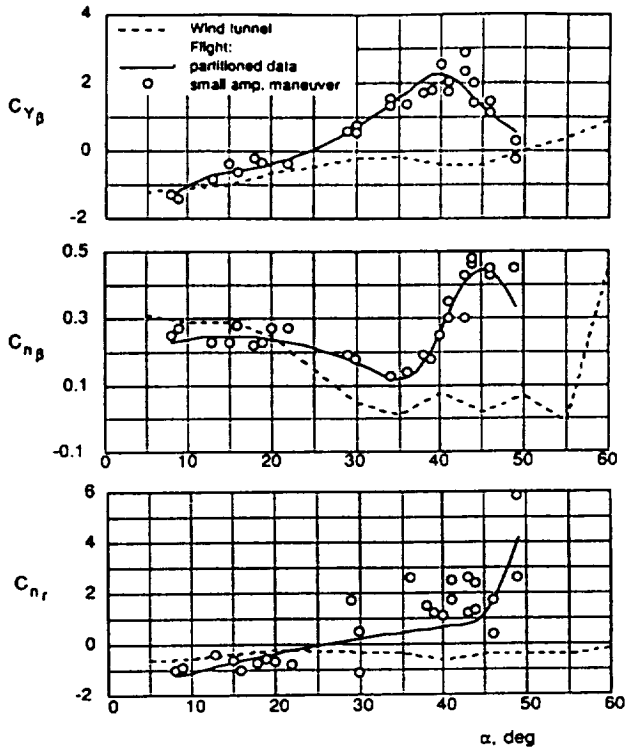

Figure 8. Comparison of lateral-force and yawing-moment parameters estimated from flight and wind-tunnel experiment.

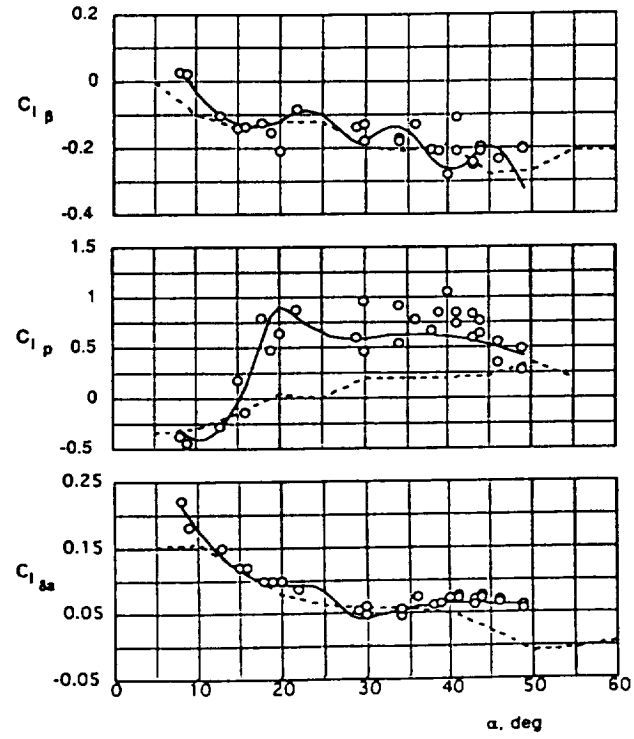

Figure 9. Comparison of rolling-moment parameters estimated from flight data and wind-tunnel experiment.

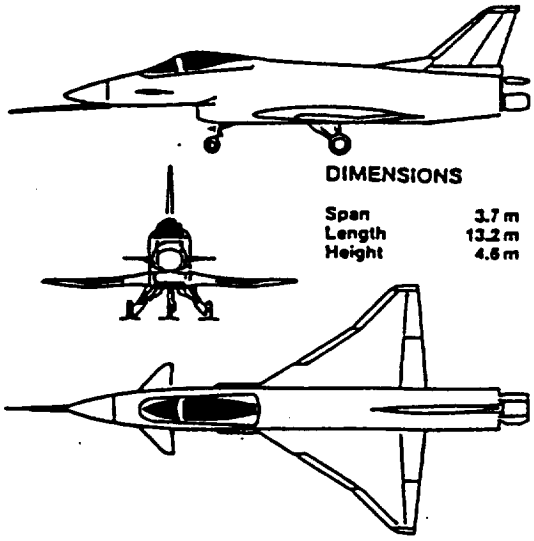

Figure 10. Drawing of X-31A aircraft.

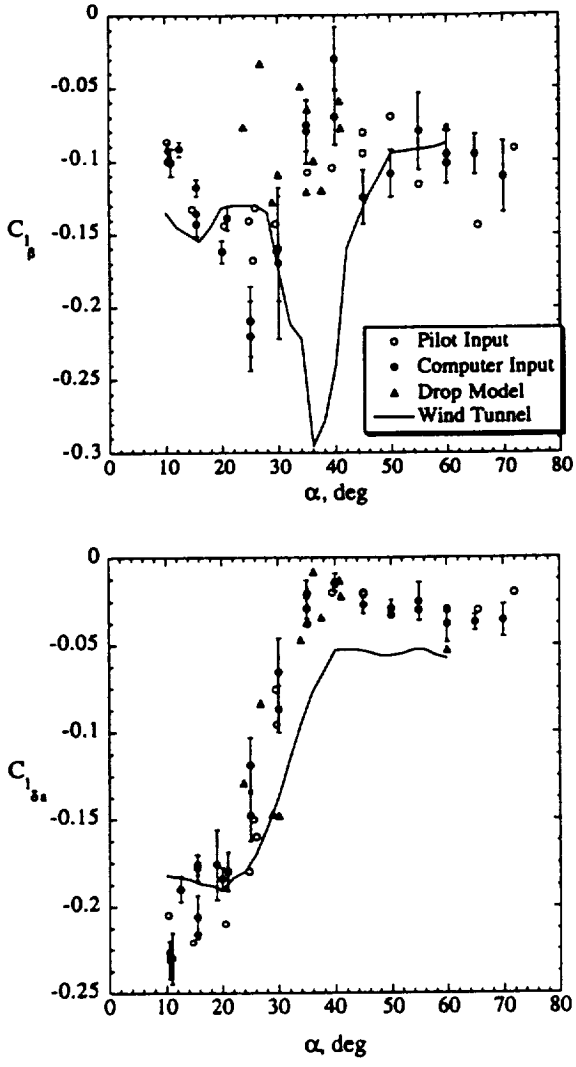

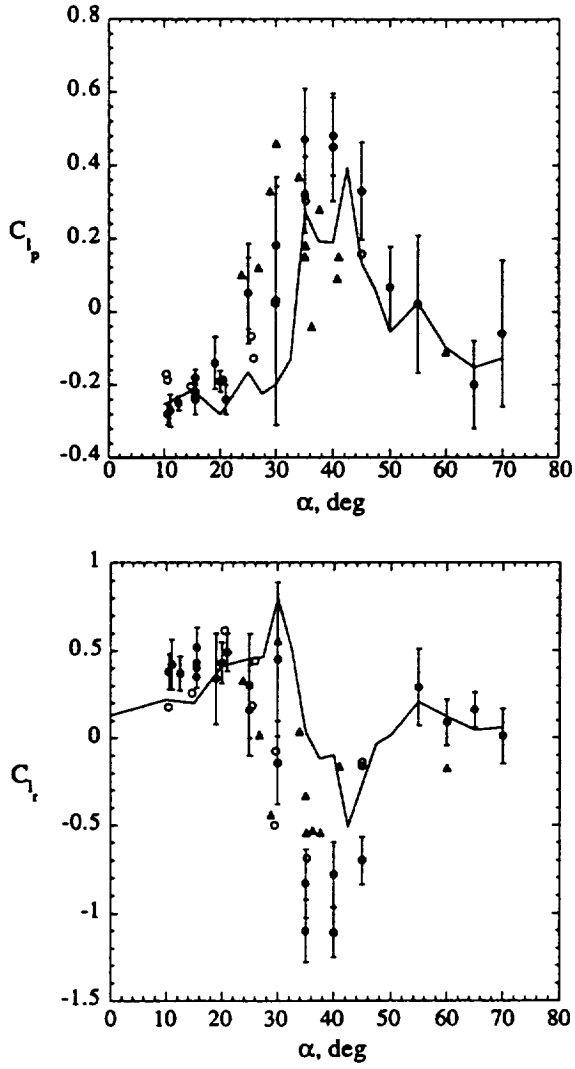

Figure 11. Comparison of rolling-moment parameters estimated from full-scale aircraft and drop model data, and wind-tunel experiment.

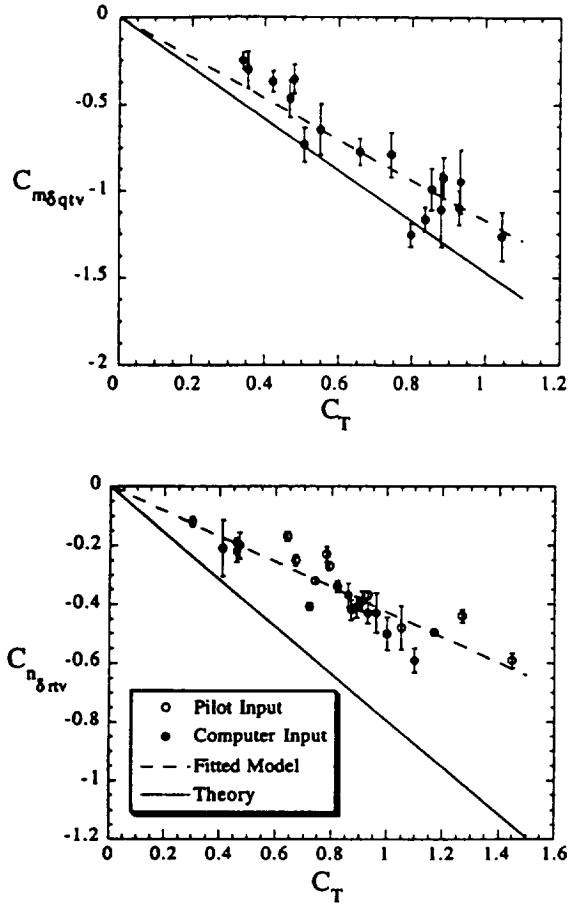

Figure 12. Comparison of estimated thrust- vectoring effectiveness and its theoretical values.

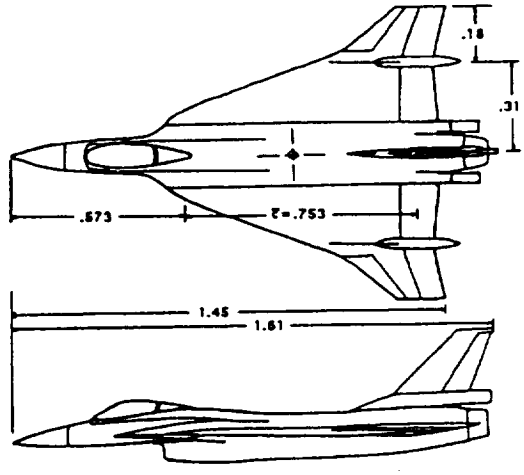

Figure 13. Drawing of F-16XL model.

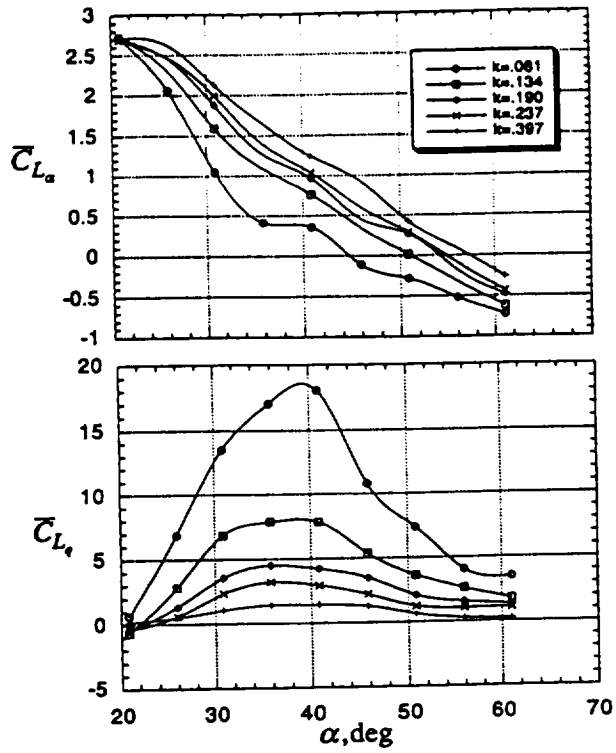

Figure 14. Variation of in-phase and out-of-phase components with angle of attack for different values of reduced frequency.

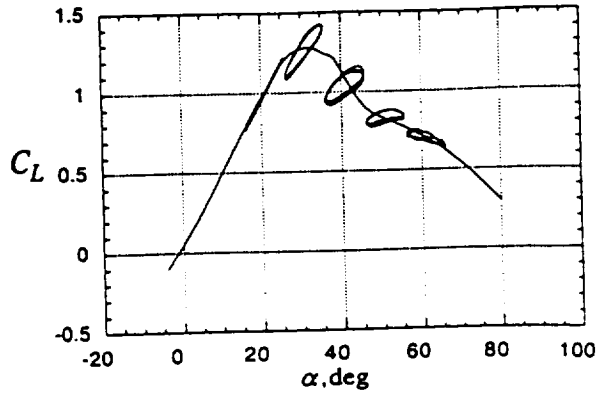

Figure 15. Lift coefficient obtained from static and oscillatory data for k=0.190.

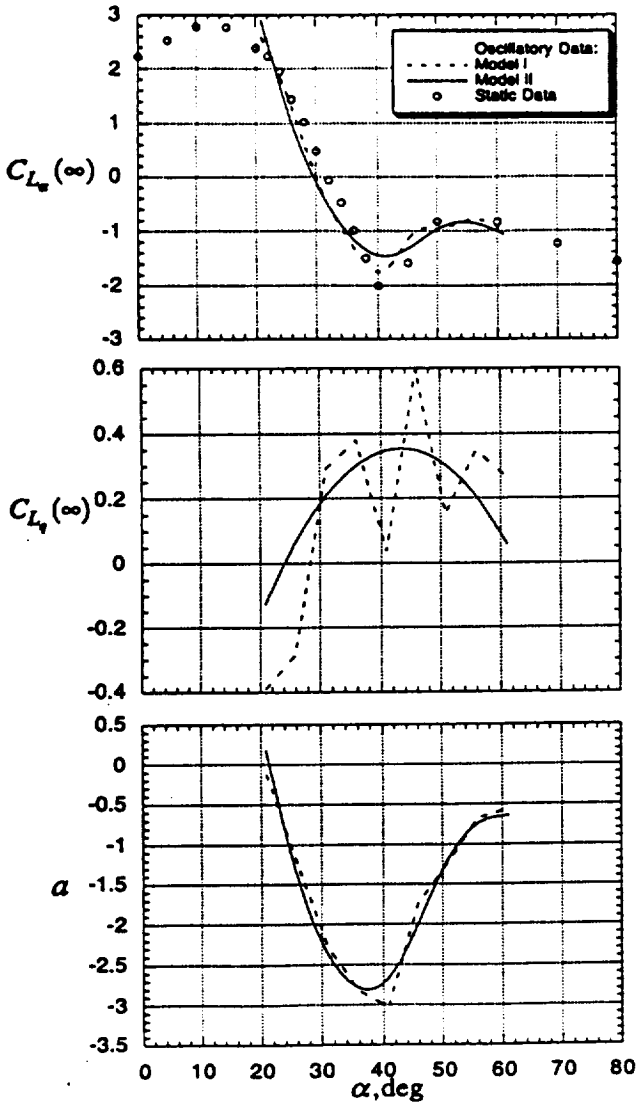

Figure 16. Estimated parameters of lift components.

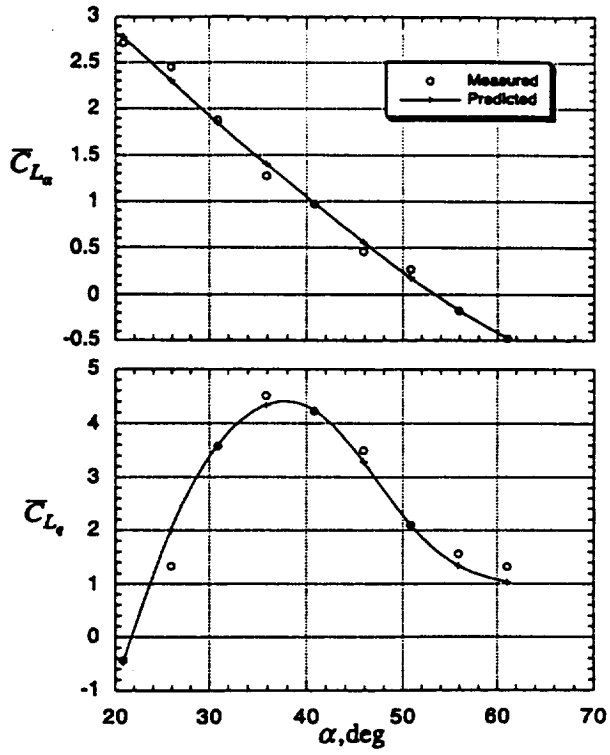

Figure 17. Measured and predicted in-phase and out-of-phase components of lift coefficient. Model II, k=0.190.